CrossMark

ORIGINAL ARTICLE

# MiR-141 Inhibits Gastric Cancer Proliferation by Interacting with Long Noncoding RNA MEG3 and Down-Regulating E2F3 Expression

Xiaoying Zhou[1,2] · Guoping Ji[1,2] · Xiquan Ke[3] · Huiyuan Gu[4] · Wujuan Jin[1,2] · Guoxin Zhang[1,2]

**Abstract**

*Background* MiR-141 and long noncoding RNA MEG3 have been independently reported to be tumor suppressor genes in various cancers. However, their expression has never been previously associated with gastric cancer (GC).
*Aims* To investigate the interaction of miR-141 and MEG3 in GC.
*Methods* QRT-PCR was used to detect miR-141, MEG3, and E2F3 in gastric tissues and cells. CCK-8 and flow cytometry analysis were used to detect cell functions. Western blot and luciferase activity were used to identify E2F3 as one of the direct targets of miR-141.
*Results* We found that expression of both miR-141 and MEG3 was significantly reduced in GC compared with levels in matched nonmalignant tissues. Positive correlation between miR-141 and MEG3 was found in both tumor tissues and control tissues. Furthermore, the over-expression of either miR-141 or MEG3 in 7901 and MKN45 cells inhibited cell proliferation and cell cycle progression and promoted cell apoptosis. E2F3 was identified as a target of miR-141, and its inhibition significantly reduced MEG3 expression. E2F3 expression was also found to be negatively associated with both MEG3 and miR-141. E2F3 over-expression partly reversed the changes caused by transfection of miR-141 mimic, and inhibition of miR-141 or MEG3 overrides MEG3- or miR-141-induced modulation of cell growth in GC.
*Conclusions* These findings together suggested that miR-141 could be interacting with MEG3 and targeting E2F3, and these factors may play important anti-tumor effects in GC pathogenesis and provide therapeutic targets in the clinics.

**Keywords** MiR-141 · MEG3 · Cell growth · Cell cycle · Gastric cancer

Xiaoying Zhou, Guoping Ji, and Huiyuan Gu have contributed equally to this work.

✉ Guoxin Zhang
15850668395@163.com

1 Department of Gastroenterology, First Affiliated Hospital of Nanjing Medical University, Nanjing 210029, China

2 First Clinical Medical College of Nanjing Medical University, Nanjing 210029, China

3 Department of Gastroenterology, First Affiliated Hospital, School of Medicine, Xi'an Jiaotong University, Xi'an 710061, Shanxi, China

4 Department of Gastroenterology, First Affiliated Hospital of Soochow University, Suzhou, China

## Introduction

From a worldwide perspective, gastric cancer (GC) is the fourth most common malignant cancer and the second leading cause of cancer-related deaths, especially in Asia [1]. Despite recent improvements in surgery and chemotherapy, the prognosis for gastric cancer remains grim [2]. Therefore, a better understanding of the molecular mechanisms and evaluation of new therapeutic strategies for this disease is required.

Differentially expressed genes identified from hundreds of cancer profiling studies over the last several years have yielded numerous biomarkers that have improved the subtyping, classification, and diagnosis of tumors for both research and clinic [3]. However, the human transcriptome comprises not only large numbers of protein-coding

messenger RNAs (mRNAs), but also a large set of noncoding RNAs (ncRNAs) that have structural, regulatory, or unknown functions [4]. Emerging evidence demonstrates that deregulated microRNAs (miRNAs) are involved in many processes of tumor progression, such as tumor initiation, cell proliferation, apoptosis, invasion, metastasis, angiogenesis, and epithelial-to-mesenchymal transition [5]. We and other groups have found that a number of miRNAs, including miR-375 [6], miR-204 [7], and miR-126 [8], were down-regulated in GC. In contrast, long noncoding RNAs (lncRNAs), tentatively defined as ncRNAs more than 200 nt in length, are also known to play key roles in cancer development and aberrant expression of lncRNAs have been functionally associated with GC [9]. Recent studies have found that lncRNAs might play as competing endogenous RNAs (ceRNAs) to exert their function on tumors, by binding with MREs and inhibiting target gene expression [10]. However, the relationship between miRNA and lncRNA and their role in GC remained largely unknown.

In this study, GC tumor samples revealed that both miR-141 and MEG3 were down-regulated compared with matched nonmalignant tissues. We hypothesized that reduced miR-141 expression could potentially represent a mechanism for the silencing of MEG3 through the modulation of E2F3 activity. We therefore sought to examine the aspects of the molecular functions of miR-141 and MEG3 in GC cell models.

## Materials and Methods

### Human Tissue Specimens

Seventy-five GC samples and 75 histological normal gastritis tissues were obtained from patients who were admitted to the Department of Gastroenterology of Nanjing Medical University between May 2013 and March 2014. Tumor tissues and gastritis tissues that were at least 1.5 cm distal to the tumor margins were snap-frozen in liquid nitrogen and then stored at −80 °C until use. All of the freshly frozen blocks of surgical samples were carefully dissected by the pathologists using H&E-stained sections as a template to identify areas containing at least 70 % tumor or normal cells. The study was approved by the Institutional Ethics Committee of Nanjing Medical University. The experiments were undertaken with the understanding of Declaration of Helsinki, and written consent was obtained from each patient.

### RNA Isolation and Quantitative Reverse Transcription PCR (qRT-PCR)

Total RNA was isolated from tumor and normal tissue samples by using TRIzol reagent (Takara, Japan) according

to the manufacturer's instructions. The expression of miR-141 was determined by quantitative stem-loop reverse transcription qRT-PCR. Primers for qRT-PCR of miR-141, MEG3, E2F3, U6 (internal control for miRNA), and β-actin (internal control for lncRNAs) are listed in Supplementary Table 1. Quantitative PCR was conducted at 95 °C for 10 min followed by 40 cycles of 95 °C for 15 s and 60 °C for 60 s in an ABI StepOne real-time PCR system. The relative expression levels of miR-141 and MEG3 were calculated with $2^{-\Delta\Delta C_t}$ method. The data were presented as the fold change of miR-141 or MEG3 expression in tumor tissues compared with their adjacent nonmalignant tissues (T/N).

### Cell Cultures and Transfection

An immortalized human gastric epithelial cell line GES-1 was cultured in RPMI 1640 (Gibico) medium supplemented with 15 % fetal bovine serum (FBS), as described previously. The human GC cell lines MKN45 and 7901 and embryonic kidney cell HEK-293T were cultured in RPMI-1640 (Hyclone, USA). MiRNAs were transfected at a working concentration of 100 nmol/L using Lipofectamine 2000 reagent (Invitrogen, USA). The miR-141 mimic, a nonspecific miR control, miR-141 inhibitor, a nonspecific miR inhibitor control, pcDNA-E2F3, and pcDNA control were all purchased or generated from GenePharma (Shanghai, China).

### MiRNA Target Validation

E2F3 was identified as miR-141 target in TargetScan. 3′UTR (untranslated regions) was amplified by PCR and cloned downstream of the firefly luciferase gene in pGL3 vector (Promega). The vector was named wild-type (wt) 3′UTR. Site-directed mutagenesis of the miR-141 binding site in E2F3 3′UTR was generated by Invitrogen, which is named mutant (mt) 3′UTR. For reporter assays, wt or mt 3′UTR vector and the control vector pRL-CMV (Renilla luciferase, Promega) were co-transfected. Luciferase activity was measured 36 h after transfection using the Dual-Luciferase Reporter Assay System (Promega).

### Western Blot Analysis

Cells were lysed in RIPA lysis buffer and extracted proteins. They were subjected to 10 % SDS-polyacrylamide gel electrophoresis and transferred to polyvinylidene difluoride membrane (Millipore). Membranes were incubated with primary antibodies at 4 °C overnight and washed extensively, followed by incubation with horseradish peroxidase-conjugated second antibodies at room

temperature for 1 h and detected with the ECL kit (Thermo). The primary antibodies against E2F3 (Cell Signaling Technology) and β-actin (Cell Signaling Technology) were diluted 1:1000. To quantify the bands obtained through Western blot analysis, we applied ImageJ software-based analysis. The background was subtracted, and the signals of the detected bands were normalized to the amount of loading control β-actin band.

## Cell Proliferation Assays

The effects of miR-141 and MEG3 over-expression on SGC-7901 and MKN45 cells proliferation were assessed using the Cell Counting Kit-8 (CCK-8, Dojindo, Kumamoto, Japan). Briefly, the cells were seeded into 96-well plates ($2 \times 10^3$ cells/well). After transfection, CCK-8 (10 μL) was added to each well at various time points and incubated at 37 °C for 3 h. The absorbance at 450 nm was measured using a microplate spectrophotometer (Bio-Tek Instruments Inc., Winooski, VT, USA).

## Cell Cycle and Apoptosis Analysis

SGC-7901 cells were transfected with pcDNA3.1, miR-141 mimics, or pcDNA3.1-MEG3, respectively. At 48 h post-transfection, cells were harvested by trypsin and washed with phosphate-buffered saline (PBS). For cell cycle analysis, the cells were fixed with 75 % ethanol at 4 °C overnight. On the following day, fixed cells were washed with PBS, treated with RNase A (50 μg/mL) in PBS at 37 °C for 20 min, and then mixed with propidium iodide (PI, 50 μg/mL) for 30 min in the dark. The stained cells were analyzed with fluorescence-activated cell sorting (FACS) by flow cytometry (FACSCalibur, Becton–Dickinson, Bedford, MA, USA). The cell debris and fixation artifacts (aggregates of cells) were gated out, and cell populations that were at the G0/G1, S, and G2/M phases were quantified using the ModFit software (Becton–Dickinson). At least 10,000 cells in each sample were analyzed to obtain a measurable signal. For apoptosis analysis, an Annexin-V-FLUOS Staining kit (Roche, Mannheim, Germany) was used according to the manufacturer's instructions 48 h after transfection. Apoptosis was analyzed with FACS using the CellQuest software (Becton–Dickinson). Annexin-V-FLUOS-positive cells were regarded as apoptotic cells.

## Statistical Analysis

Student's *t* test was used to analyze the relationship between miR-141 and MEG3 expression. Correlation between the expression of miR-141 with MEG3 and E2F3 with miR-141/MEG3 was analyzed using Pearson's rank correlation coefficient analysis. All statistical analyses were performed using SPSS 17.0. Experiments with cell cultures were done at least in triplicate. Data were expressed as mean ± standard deviation (SD). A two-tailed value of $p < 0.05$ was considered to be statistically significant.

# Results

## MiR-141 and MEG3 Expression Were Decreased in GC and Were Correlated with Cancer Progression

We evaluated the expression levels of miR-141 and MEG3 in 75 pairs of GC and the histologically normal gastritis tissues. Statistically, the average expression levels of miR-141 (Fig. 1a) and MEG3 (Fig. 1b) were significantly down-regulated in tumor tissues. Moreover, miR-141 (Fig. 1c) and MEG3 (Fig. 1d) expression levels were also significantly decreased in the GC cell lines 7901 and MKN45, compared with immortalized gastric epithelial cell GES-1. The relationships between miR-141 expression, MEG3 expression, and the clinicopathological factors of GC are presented in Table 1. By normalizing miR-141 and MEG3 expression levels in the tumor tissues with adjacent nonmalignant tissues, miR-141 expression (T/N) was significantly correlated with metastasis and clinical stage and MEG3 expression (T/N) was significantly correlated with tumor size and clinical stage. Besides, we also divided the control gastritis tissues according to *H. pylori* infection state. There were 31 *H. pylori*-positive and 44 *H. pylori*-negative patients. We found that miR-141 expression was significantly decreased in *H. pylori*-positive tissues ($p < 0.05$), while MEG3 expression showed no difference between the two groups ($p > 0.05$).

## Expression of MiR-141 Was Positively Correlated with MEG3 Expression in Clinical Specimens

Because both miR-141 and MEG3 were shown to be correlated with cancer progression, we examined the relationship of their expression levels using Pearson's rank correlation coefficient analysis. We found that the expression level of miR-141 was positively correlated with MEG3 expression in both GC ($R = -0.889$, $p = 0.001$, Fig. 1e) and matched nonmalignant tissues ($R = -0.866$, $p = 0.000$, Fig. 1f).

## Over-Expression of Either MiR-141 or MEG3 in GC Cells Inhibited Cell Proliferation and Cell Cycle Progression and Promoted Apoptosis

The expression of miR-141 and MEG3 was significantly increased in SGC-7901 and MKN45 cells after transfection with pcDNA3.1-MEG3 or miR-141 mimics compared with

**Fig. 1** Expression of miR-141 and MEG3 in GC. **a, b** MiR-141 and MEG3 were reduced in human 75 GC tissues compared with matched adjacent tissues. **c, d** MiR-141 and MEG3 were reduced in MKN45 and 7901 cell lines, as compared with immortalized GES-1 cells. **e, f** Positive correlation between miR-141 and MEG3 expression levels in GC and matched nonmalignant tissues
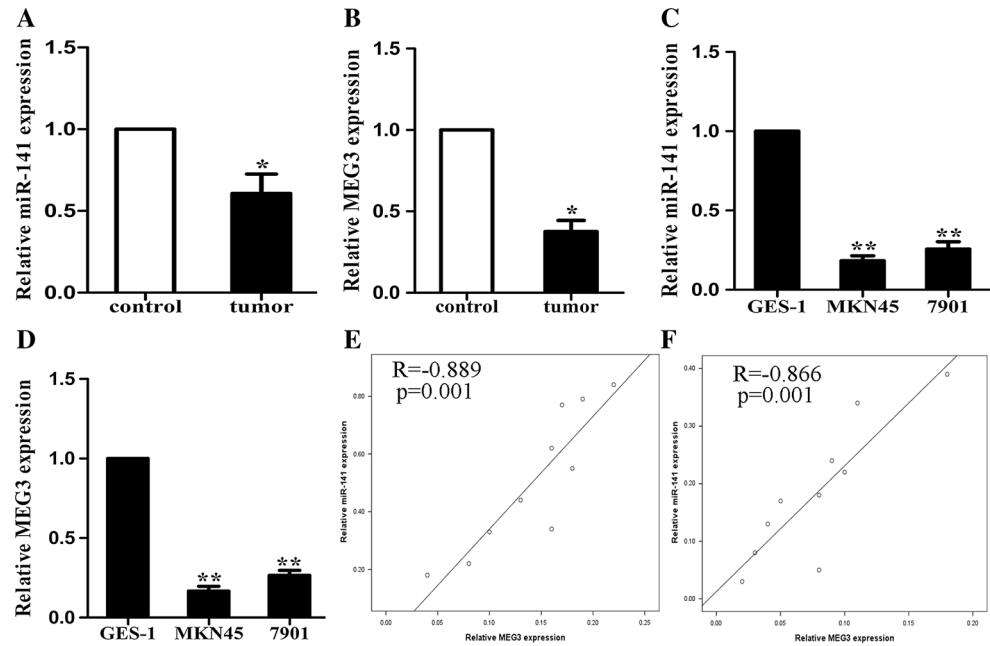


**Table 1** Relationship between expression of miR-141 and MEG3 and clinicopathologic factors in 75 GC patients

| Characteristics | No. | MiR-141 (T/N) | | MEG3 (T/N) | |
|---|---|---|---|---|---|
| | | Mean ± SD | $p$ | Mean ± SD | $p$ |
| Sex | | | 0.775 | | 0.864 |
| Male | 40 | 0.776 ± 0.341 | | 0.441 ± 0.255 | |
| Female | 35 | 0.787 ± 0.318 | | 0.429 ± 0.452 | |
| Age | | | 0.434 | | 0.628 |
| <50 years | 39 | 0.752 ± 0.847 | | 0.418 ± 0.691 | |
| ≥50 years | 36 | 0.814 ± 0.441 | | 0.450 ± 0.772 | |
| Tumor size | | | 0.223 | | 0.002** |
| T1–T2 | 44 | 0.835 ± 0.359 | | 0.607 ± 0.348 | |
| T3–T4 | 31 | 0.729 ± 0.288 | | 0.269 ± 0.532 | |
| Metastasis | | | 0.031* | | 0.062 |
| Yes | 34 | 0.609 ± 0.633 | | 0.369 ± 0.237 | |
| No | 41 | 0.950 ± 0.466 | | 0.499 ± 0.223 | |
| Clinical stage | | | 0.048* | | 0.012* |
| I–II | 45 | 0.911 ± 0.434 | | 0.592 ± 0.321 | |
| III–IV | 30 | 0.652 ± 0.532 | | 0.279 ± 0.134 | |

\* $p < 0.05$, \*\* $p < 0.01$

transfection with controls (Fig. 2a). We examined the cellular effects of the independent restoration of miR-141 and of MEG3 expression on cell growth and proliferation in the SGC-7901 and MKN45 cell models of GC. Over-expression of either miR-141 or MEG3 significantly inhibited the viability of GC cells (Fig. 2b). Over-expression of either factor also leaded to substantial accumulation of the cell populations at the G1 stage of the cell cycle (Fig. 2c). MiR-141 mimic or pcDNA-MEG3 could also promote cell apoptosis (Fig. 2d), revealing that miR-141

**Fig. 2** Over-expression of miR-141 and MEG3 inhibits cell viability ▶ and cell progression, while promoting cell apoptosis. Cells were transfected with negative control (NC) or miR-141 mimics or pcDNA-MEG3 or pcDNA-NC, as indicated. **a** Relative expression of miR-141 or MEG3 after transfection validated by qRT-PCR. **b** Over-expression of miR-141 and MEG3 inhibits cell viability. Cell viability was measured using CCK-8 assays. **c** Inhibition of cell cycle progression by over-expression of miR-141 or MEG3. Cells were stained with propidium iodide (PI) at 48 h posttransfection and analyzed with FACS. **d** Promotion of apoptosis by over-expression of miR-141 or MEG3. Cells were transfected for 48 h, and apoptosis cells were monitored with FACS after Annexin-V and PI staining. Data were presented as mean ± SD
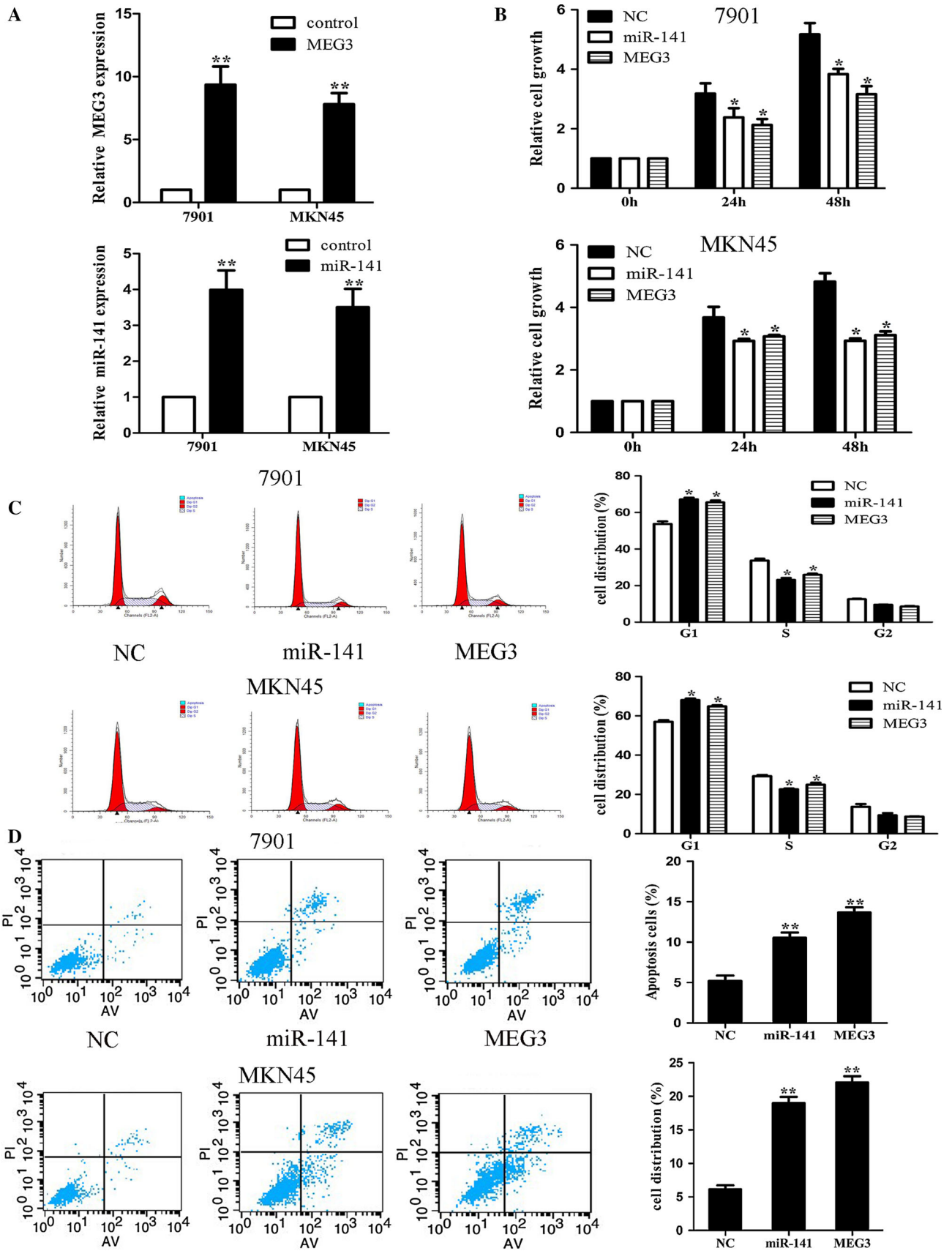
and MEG3 have marked anti-tumorigenic cellular functions in GC.

## Over-Expression of MiR-141 Decreased Expression of E2F3 by Targeting the 3′UTR of Its mRNA and Increased MEG3 Expression

The mRNA for E2F3 contains one conserved putative miR-141 target site in its 3′UTR according to two of the most commonly used software algorithms (TargetScan and MiRanda; Fig. 3a). Therefore, we constructed luciferase reporter plasmids to contain either the wild-type or the mutated miR-141 target sequences in the 3′UTR of E2F3. Both the wild-type and the mutant reporters were introduced into HEK-293T cell. We found that ectopic expression of miR-141 suppressed the luciferase activity of the reporters containing E2F3 3′UTR, but not the reporter vector containing the mutation of the miR-141 binding site (Fig. 3b). In addition, we examined the effects of over-expression/down-regulation of miR-141 on the endogenous expression of E2F3 protein in SGC-7901 cells by Western blot and qRT-PCR analysis. The expression of both E2F3 protein and mRNA was significantly decreased in GC cells in which miR-141 mimic transfected, in comparison with same cells transfected with negative control, and E2F3 was over-expressed when miR-141 inhibitor transfected (Fig. 3c). We detected MEG3 expression by qPCR analysis in cells transfected with miR-141 mimics/inhibitor. We found that MEG3 expression was significantly over-expressed when transfecting with miR-141 mimics and decreased when transfecting with miR-141 inhibitor (Fig. 3d). We also examined the effect of knockdown the E2F3 expression on MEG3 expression by siRNAs. As shown in Fig. 3e, E2F3 mRNA and protein level were significantly suppressed by siRNA transfection. We found that E2F3 knockdown induces MEG3 expression in GC cells (Fig. 3f). These findings suggested that miR-141 could increase MEG3 expression through reduction in the expression of E2F3 in vitro.

## Expression of E2F3 Was Inversely Correlated with MiR-141 and MEG3 Expression in GC

We sought to confirm the molecular relationship observed between E2F3 activity and expressed levels of miR-141 and MEG3 in patient's GC tissues and cells. Correlation between E2F3, MEG3, and miR-141 expression was examined in 15 pairs of randomly selected GC tissues by qRT-PCR analysis. The E2F3 mRNA expression was up-regulated in GC compared with matched nonmalignant tissues (Fig. 4a) and consistent with the result that E2F3 mRNA expression was increased in 7901 and MKN45 cell lines, compared with immortalized GES-1 cells (Fig. 4b).

Pearson's correlation coefficient analysis suggested that relative E2F3 expression (T/N) was inversely correlated with miR-141 (Fig. 4c, $R = -0.752$, $p = 0.012$) and MEG3 (Fig. 4d, $R = -0.686$, $p = 0.028$) expression.

## Transfection of pcDNA-E2F3 Partly Reversed the Changes Caused by Transfection of hsa-miR-141 Mimic

The increased expression of E2F3 protein was observed after cells transfected with E2F3 by Western blot. E2F3 expression was significantly higher in cells co-transfected with miR-141 mimics and E2F3, compared with control and cell transfected with miR-141 mimics alone (Fig. 5a). The co-transfection partly reversed cell proliferation inhibition induced by miR-141 transfection (Fig. 5b). Also, the co-transfection significantly decreased cells in G1 phase and increased cells in S and G2 phases, which suggested that G1-phase arrest by miR-141 was partially reversed by E2F3 transfection (Fig. 5c).

## Expression of MiR-141 or MEG3 Rescued MEG3- or MiR-141-Induced Modulation of Cell Growth in GC

Having demonstrated the relationship between lncRNA MEG3 and miR-141 by our present data, we further explore the importance of miR-141 or MEG3 in MEG3- or miR-141-mediated cell growth. Western blot analysis showed that MEG3 transfection could significantly reduce E2F3 expression and that after cell co-transfecting with MEG3 and miR-141 inhibitor, the E2F3 protein expression was restored (Fig. 6a). Also, miR-141 inhibitor could restore significantly cell growth repressed by MEG3 over-expression (Fig. 6b). Furthermore, miR-141 inhibitor reduced cell G1-phase arrest induced by MEG3 (Fig. 6c). Similar results are found in Fig. 7, which shows that MEG3 siRNA could reverse cell growth effect and distribution induced by miR-141.

## Discussion

The present study is a comprehensive combined analysis of microRNA and lncRNA expressions in patient's GC samples and their matched nonmalignant tissues, which was reported for the first time. It was found that miR-141 and long noncoding RNA MEG3 were reduced in GC compared with control, confirmed in 75 pairs of tissues by qRT-PCR analysis. The reduction in miR-141 and MEG3 has been reported to occur in a variety of tumors including GC [11, 12], hepatocellular carcinoma [13, 14], and bladder cancer [15, 16]. These reported findings suggested potential

**Fig. 3** MiR-141 can increase the MEG3 expression through reducing the expression of E2F3. **a** The seed sequence of miR-141 (*middle*) matches the 3′UTR of E2F3 (*top*). Mutations introduced into the 3′UTR of E2F3 (*bottom*). **b** miR-141 inhibited wild-type, but not mutated, E2F3 3′UTR luciferase reporter activity. Cells were co-transfected with firefly luciferase reporter plasmids containing wild-type or mutant 3′UTR of E2F3. **c** Inhibition of the protein expression of E2F3 by miR-141. Cells were transfected with miR-141 mimic or inhibitor as indicated, and E2F3 was detected by Western blot and qRT-PCR analysis. **d** Expression of miR-141 correlated with MEG3 expression. Cells were transfected with mimic or inhibitor, and MEG3 expression was detected by qRT-PCR. **e** Inhibition of E2F3 protein and mRNA expression by siRNAs to E2F3 and E2F3 was detected by Western blot and qRT-PCR analysis. **f** Inhibition of E2F3 protein expression was correlated with MEG3 expression up-regulated. Cells were transfected with siRNA control, siRNA1 and siRNA2, as indicated, and MEG3 expression level was detected by qRT-PCR. (NC: negative control compared to miR-141 mimic and iNC: inhibitor negative control compared to miR-141 inhibitor)
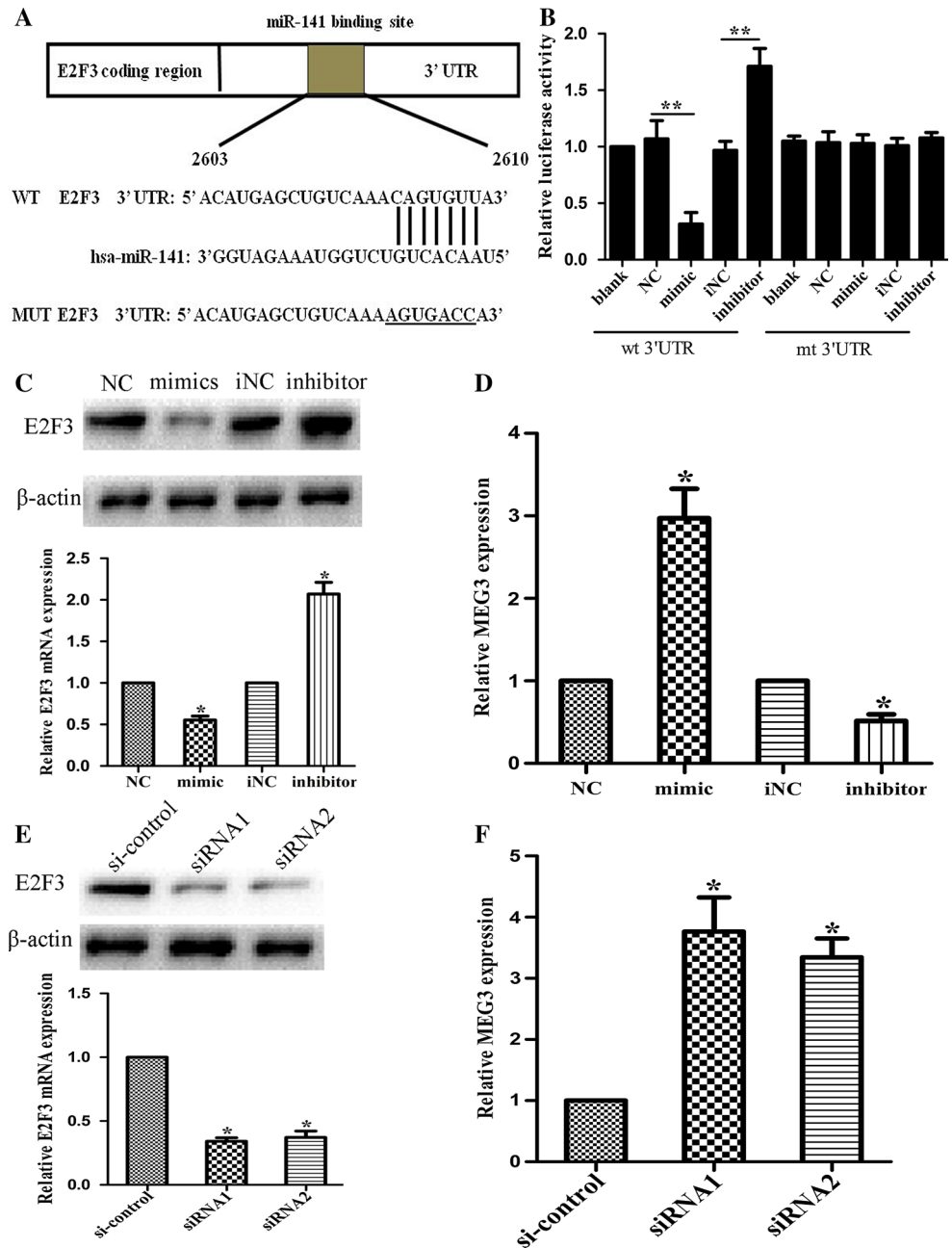
anti-tumorigenic effects for both miR-141 and MEG3 in cancer pathogenesis.

Initially, we found that both in tumor tissues and in control tissues, the expression of MEG3 was positively related to miR-141, in either tumor or adjacent control tissues ($p < 0.05$). To the best of our knowledge, there are no published reports of a relationship between the combination of miR-141 and MEG3 expression in cancer patients. After transfecting cells with miR-141 mimics/inhibitor, the expression level of MEG3 was also increased/decreased, and when we silence E2F3 expression, the expression of MEG3 was significantly higher. These findings together showed that the expression of MEG3 was regulated by miR-141.

Interestingly, others have reported evidence of another potential molecular mechanistic relationship between miR-141 and MEG3 in which miR-141 targets repression of EZH2 expression, a subunit of the polycomb repressor complex 2 (PRC2), in prostate cancer [17], while MEG3 has been shown to interact with EZH2 in embryonic stem cells (ES cells) [18]. However, no direct relationship between the expression of miR-141 and MEG3 has been reported previously. Yet, a relationship between the expression of miR-29a and MEG3 was reported in

**Fig. 4** E2F3 was up-regulated in tumors. **a** The E2F3 expression was up-regulated in 75 pairs of tumor and control tissues by qRT-PCR. **b** The E2F3 expression was up-regulated in 7901 and MKN45 cells compared with immortalized GES-1 cells. **c** Inverse correlation between miR-141 and E2F3 expression levels in GC tissues. **d** Inverse correlation between MEG3 and E2F3 expression levels in GC tissues (*$p < 0.05$)
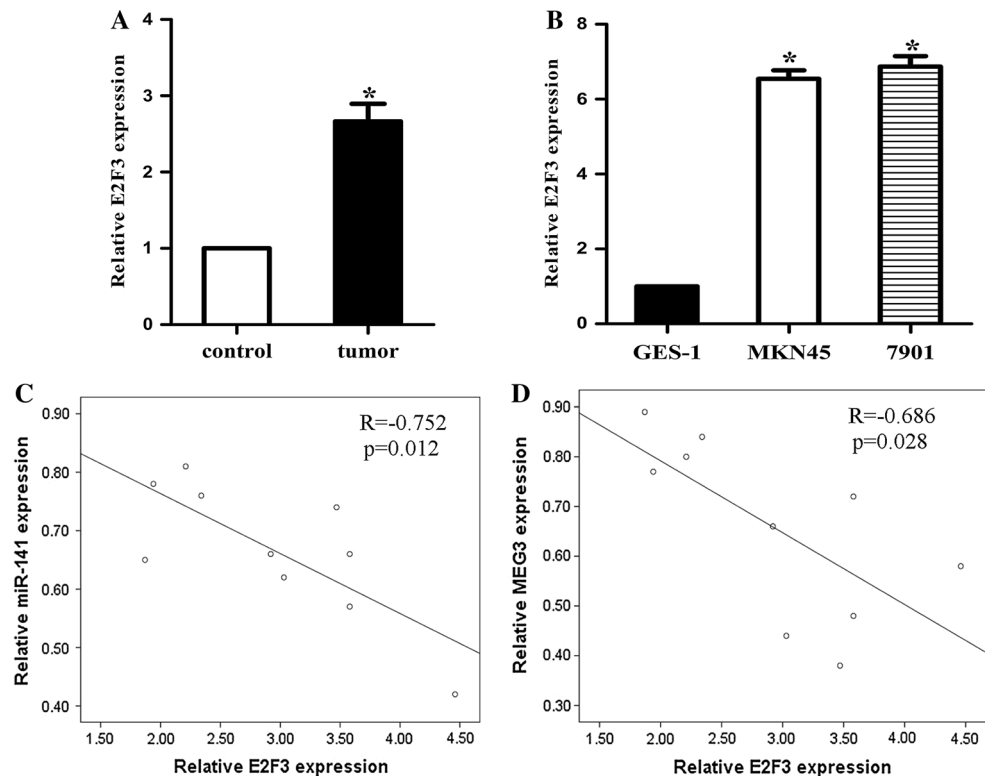
hepatocellular cancer [19], and although miR-141 is down-regulated in hepatocellular cancer, reportedly through the up-regulation of EMT inducers [20], miR-141 can also affect the pathogenesis of hepatocellular cancer by targeting the EMT pathway. In this study, molecular analysis in GC cells showed that increased miR-141 results in increased MEG3 expression through the reduced expression of its target E2F3, highlighting an elegant interrelationship between two classes of ncRNAs, miRNA, and lncRNAs and epigenetic regulation of gene expression. Our analysis does not exclude the possibility that other potential targets of miR-141 may also govern other pathways that enhance MEG3 expression and that miR-141 may also target different molecules in different types of cancer. Certainly, we have demonstrated clearly that E2F3 is a direct of miR-141 and that inhibition of E2F3 by interfering RNAi resulted in the up-regulation of MEG3, suggesting that down-regulation of E2F3 by miR-141 might readily account for the up-regulation of MEG3. We verified these in vivo showing that the expression of E2F3 in GC tissues was inversely correlated with either miR-141 or MEG3 levels. Together, these observations provided support that E2F3 is a miR-141 target gene in GC tissues.

In this study, the expression levels of hsa-miR-141 and MEG3 were significantly down-regulated in GC tissues and cells. The possible mechanisms by which miR-141 down-regulated in GC might be that miR-141 was regulated by

certain transcriptional factor (Sp1) [23] or decreased by *H. pylori* infection [11]. MiR-141 could target with oncogene STAT4 and ZEB1 [21] to regulate GC cell functions. Our in vitro experiments with human GC cell line SGC-7901 showed that both miR-141 and MEG3 inhibited cell proliferation, induced G1-phase arrest, and promoted apoptosis and that down-regulation of hsa-miR-141 or MEG3 could have reverse effects. These findings suggested that hsa-miR-141 and MEG3 are tumor suppressors in GC. For miR-141, our data are similar to the findings in liver cancer [13], breast cancer [21], and ovarian cancer [22], in which miR-141 expression was found to be reduced. Mechanistic studies have revealed that miR-141 suppressive effects in tumor cells could act through posttranscriptional inhibition of the expression of Sp1 [23]. However, there are no studies reporting relationship between miR-141 and transcription factor E2F3. E2F3 belongs to the E2F family of transcription factors that was first described as a key regulator of cell cycle progression [24]. Subsequently, E2Fs were also found to regulate genes involved in a variety of biological processes, including apoptosis, DNA repair, differentiation, and development [25]. E2F3 exerts a critical role in gene expression control during the G1/S transition, which also has major roles in regulating cell apoptosis [26]. There is mounting evidence that dysregulation of E2F3 proteins contributes to tumor formation [27]. In this study, we were the first to find that E2F3 was
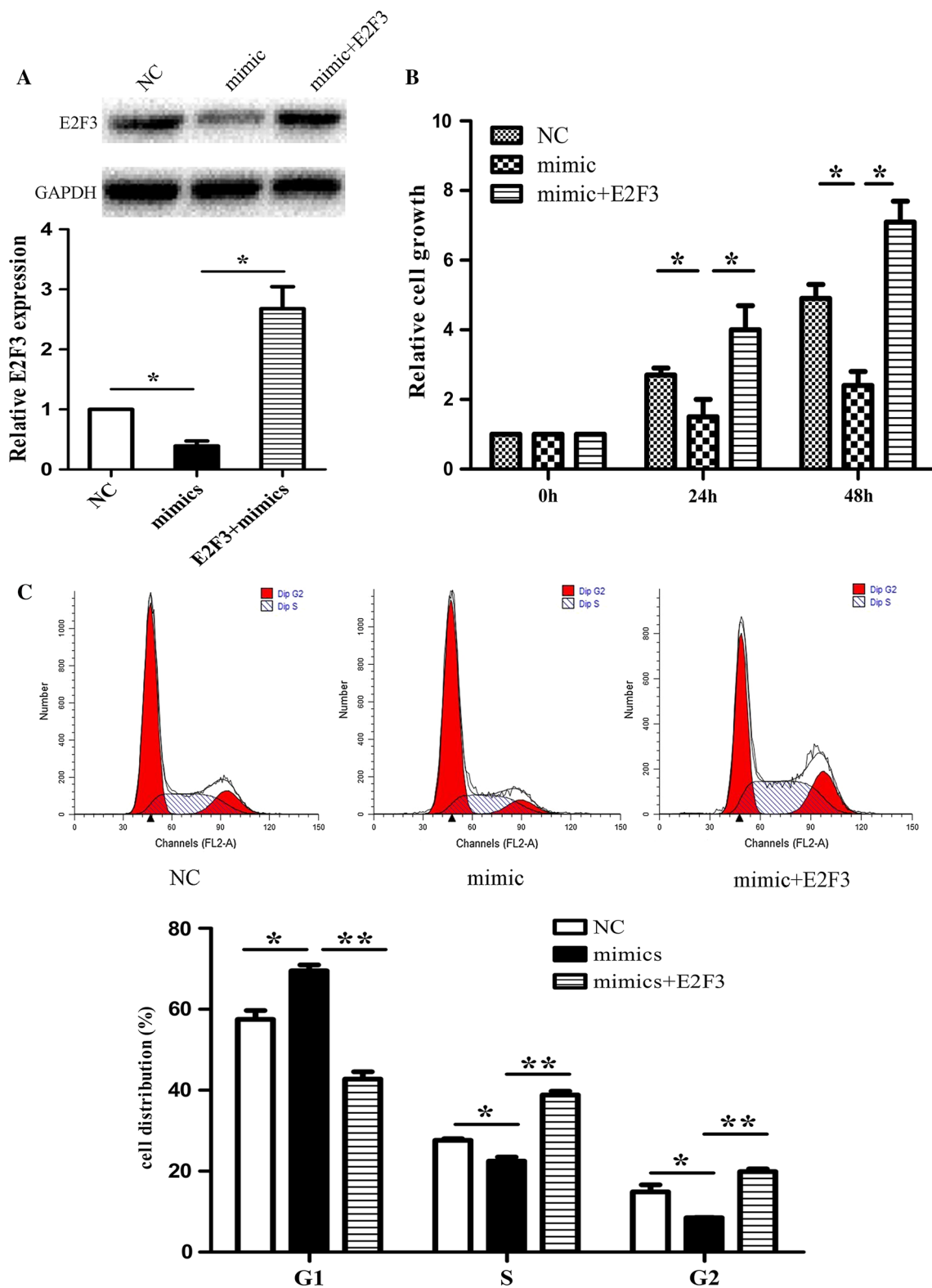
**Fig. 5** Effect of miR-141/E2F3 signaling on cell biology. **a** E2F3 expression changes following transfection with mimics and pcDNA-E2F3 were identified by Western blot analysis. **b**, **c** Effect of miR-141 mimics and pcDNA-E2F3 on cell growth and cell distribution, after differential treatment in vitro
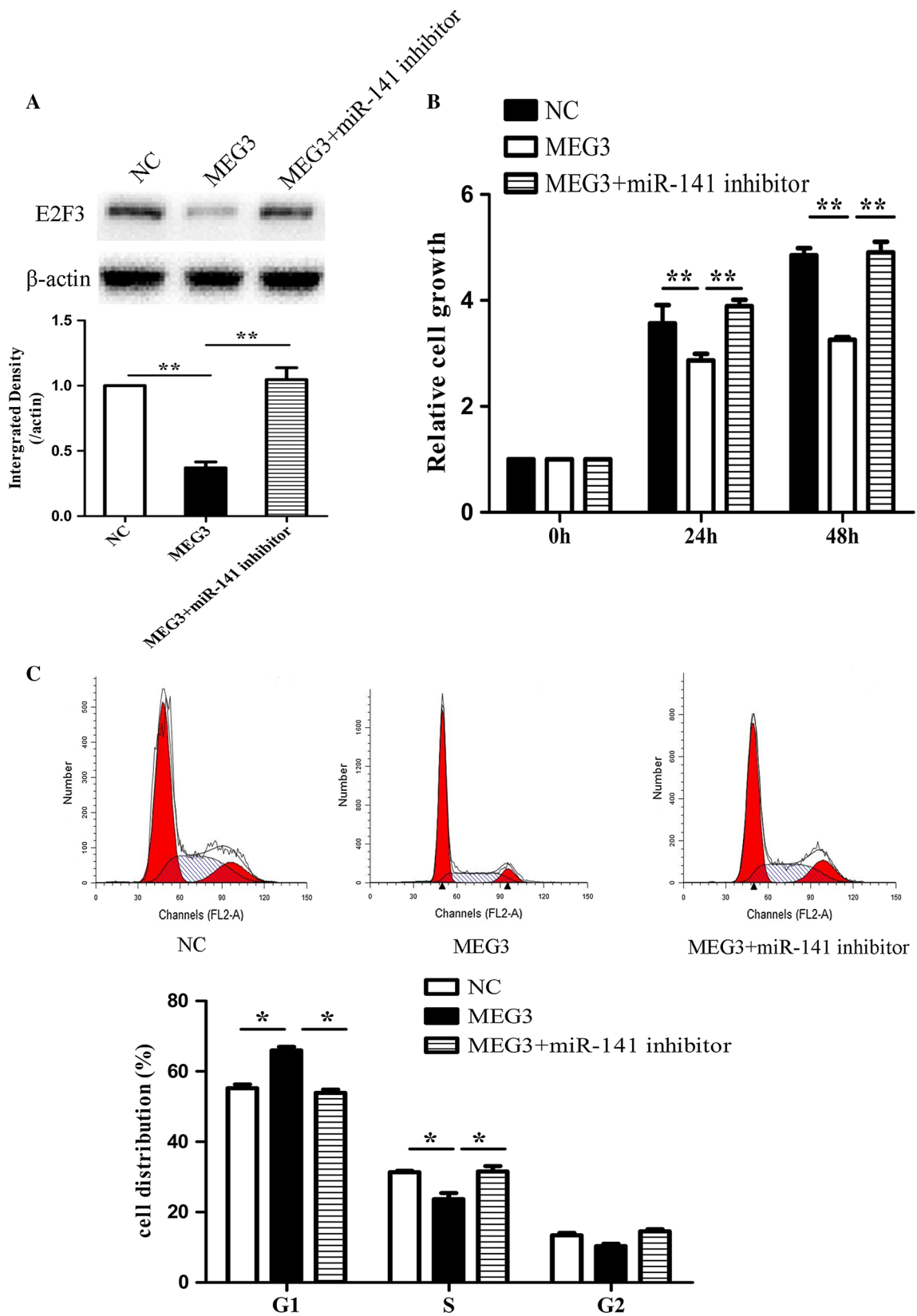
Fig. 6 Effect of miR-141 inhibitor on MEG3-induced cell growth. a E2F3 protein expression level was measured after cell transfecting with MEG3 or MEG3 with miR-141 inhibitor. b, c Effect of miR-141 inhibitor on MEG3-induced cell proliferation and cell distribution (*p < 0.05)
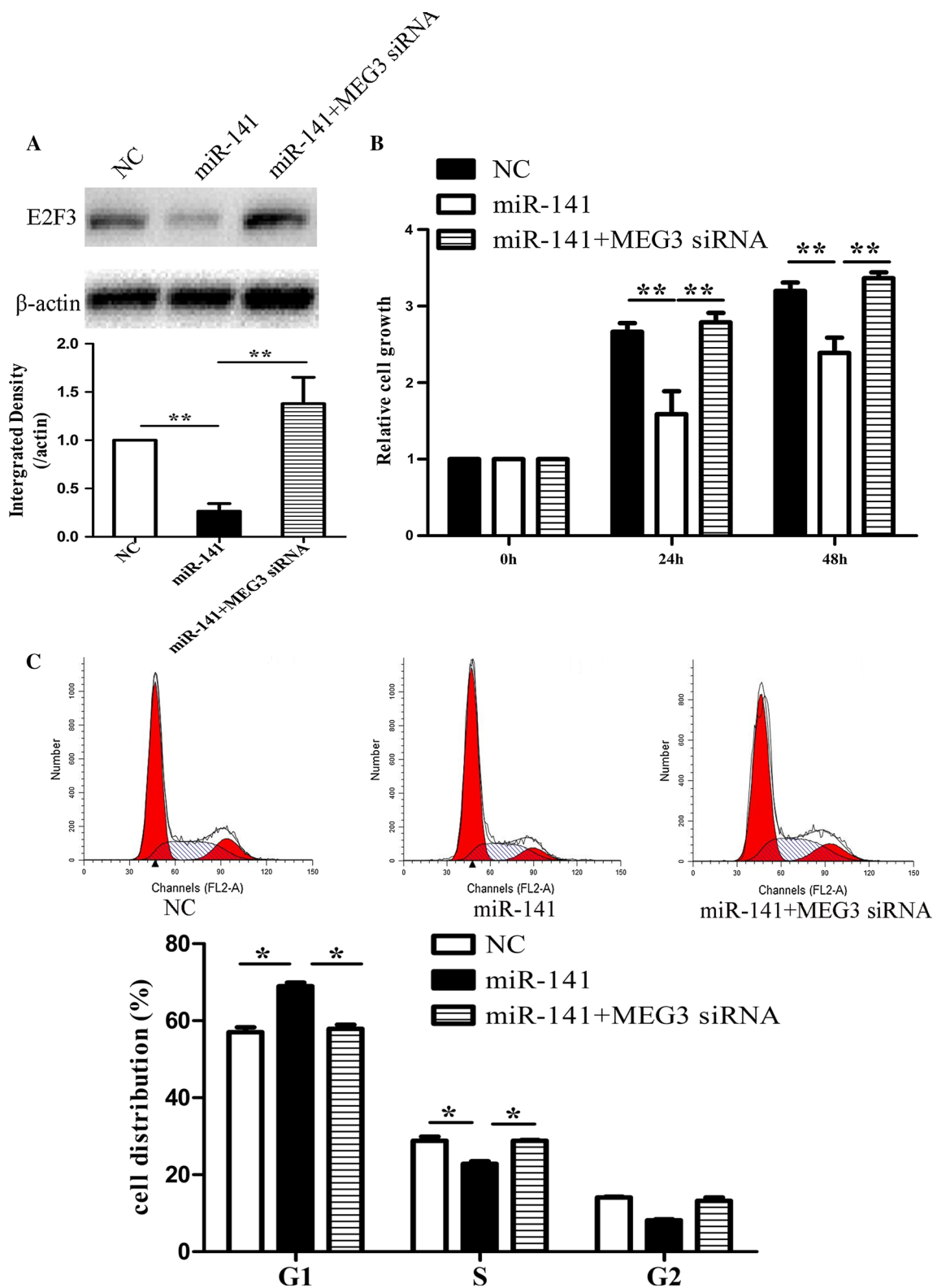
**Fig. 7** Effect of MEG3 siRNA on miR-141-induced cell growth. **a** E2F3 protein expression level was measured after cell transfecting with miR-141 or miR-141 with MEG3 siRNA. **b, c** Effect of MEG3 siRNA on miR-141-induced cell proliferation and cell distribution. (*$p < 0.05$)

one of the direct targets of miR-141 through luciferase assay and that miR-141 inhibited cell proliferation partly through repression of E2F3 expression. We co-transfected cells with miR-141 mimics and pcDNA-E2F3, compared with cell transfected with miR-141 mimics only, we found that E2F3 expression reversed miR-141 inhibition of cell proliferation and G1-phase arrest, and these results also confirmed in vivo. Together, these findings suggested that miR-141 inhibits cell growth partly through repression of E2F3 expression.

In summary, we have shown that miR-141 and MEG3 were positively correlated in tissues, that over-expression of miR-141 or MEG3 could inhibit GC cell proliferation and cycle progression and promoted cell apoptosis, and that transfecting cells with MEG3 siRNA or miR-141 inhibitor could reverse the condition, which indicated that these factors play important anti-tumor effects during GC pathogenesis and that combined miR-141 and MEG3 expression might prove useful as a therapeutic target among GC patients.

**Conflict of interest** All authors declare no potential conflict to disclose.

# References

1. Fock KM. Review article: the epidemiology and prevention of gastric cancer. *Aliment Pharmacol Ther.* 2014;40:250–260.
2. Yang W, Raufi A, Klempner SJ. Targeted therapy for gastric cancer: molecular pathways and ongoing investigations. *Biochim Biophys Acta.* 2014;1846:232–237.
3. Ma J, Hong L, Chen Z, Nie Y, Fan D. Epigenetic regulation of microRNAs in gastric cancer. *Dig Dis Sci.* 2014;59:716–723.
4. Pérez-Ortín JE, Alepuz P, Chávez S, et al. Eukaryotic mRNA decay: methodologies, pathways, and links to other stages of gene expression. *J Mol Biol.* 2013;425:3750–3775.
5. Yang YF, Wang F, Xiao JJ, et al. MiR-222 overexpression promotes proliferation of human hepatocellular carcinoma HepG2 cells by downregulating p27. *Int J Clin Exp Med.* 2014;7:893–902.
6. Miao L, Liu K, Xie M, et al. miR-375 inhibits Helicobacter pylori-induced gastric carcinogenesis by blocking JAK2-STAT3 signaling. *Cancer Immunol Immunother.* 2014;63:699–711.
7. Zhang L, Wang X, Chen P. MiR-204 down regulates SIRT1 and reverts SIRT1-induced epithelial-mesenchymal transition, anoikis resistance and invasion in gastric cancer cells. *BMC Cancer.* 2013;13:290.
8. Otsubo T, Akiyama Y, Hashimoto Y, et al. MicroRNA-126 inhibits SOX2 expression and contributes to gastric carcinogenesis. *PLoS One.* 2011;6:e16617.
9. Arita T, Ichikawa D, Konishi H, et al. Circulating long non-coding RNAs in plasma of patients with gastric cancer. *Anticancer Res.* 2013;33:3185–3193.
10. Tay Y, Rinn J, Pandolfi PP. The multilayered complexity of ceRNA crosstalk and competition. *Nature.* 2014;505:344–352.
11. Zhou X, Xia Y, Su J, et al. Down-regulation of miR-141 induced by helicobacter pylori promotes the invasion of gastric cancer by targeting STAT4. *Cell Physiol Biochem.* 2014;33:1003–1012.
12. Sun M, Xia R, Jin F, et al. Downregulated long noncoding RNA MEG3 is associated with poor prognosis and promotes cell proliferation in gastric cancer. *Tumour Biol.* 2014;35:1065–1073.
13. Yeh TS, Wang F, Chen TC, et al. Expression profile of microRNA-200 family in hepatocellular carcinoma with bile duct tumor thrombus. *Ann Surg..* 2014;259:346–354.
14. Anwar SL, Krech T, Hasemeier B, et al. Loss of imprinting and allelic switching at the DLK1-MEG3 locus in human hepatocellular carcinoma. *PLoS One.* 2012;7:e49462.
15. Ratert N, Meyer HA, Jung M, et al. miRNA profiling identifies candidate mirnas for bladder cancer diagnosis and clinical outcome. *J Mol Diagn.* 2013;15:695–705.
16. Ying L, Huang Y, Chen H, et al. Downregulated MEG3 activates autophagy and increases cell proliferation in bladder cancer. *Mol Biosyst.* 2013;9:407–411.
17. Sørensen KD, Ørntoft TF. Discovery of prostate cancer biomarkers by microarray gene expression profiling. *Expert Rev Mol Diagn.* 2010;10:49–64.
18. Zhao J, Ohsumi TK, Kung JT, et al. Genome-wide identification of polycomb-associated RNAs by RIP-seq. *Mol Cell.* 2010;40:939–953.
19. Braconi C, Kogure T, Valeri N, et al. microRNA-29 can regulate expression of the long non-coding RNA gene MEG3 in hepatocellular cancer. *Oncogene.* 2011;30:4750–4756.
20. Hur K, Toiyama Y, Takahashi M, et al. MicroRNA-200c modulates epithelial-to-mesenchymal transition (EMT) in human colorectal cancer metastasis. *Gut.* 2013;62:1315–1326.
21. Li X, Roslan S, Johnstone CN, et al. MiR-200 can repress breast cancer metastasis through ZEB1-independent but moesin-dependent pathways. *Oncogene.* 2014;3:4077–4088.
22. van Jaarsveld MT, Helleman J, Boersma AW, et al. miR-141 regulates KEAP1 and modulates cisplatin sensitivity in ovarian cancer cells. *Oncogene.* 2013;32:4284–4293.
23. Al-Khalaf HH, Mohideen P, Nallar SC, et al. The cyclin-dependent kinase inhibitor p16INK4a physically interacts with transcription factor Sp1 and cyclin-dependent kinase 4 to transactivate microRNA-141 and microRNA-146b-5p spontaneously and in response to ultraviolet light-induced DNA damage. *J Biol Chem.* 2013;288:35511–35525.
24. Julian LM, Vandenbosch R, Pakenham CA, et al. Opposing regulation of Sox2 by cell-cycle effectors E2f3a and E2f3b in neural stem cells. *Cell Stem Cell.* 2013;12:440–452.
25. Prost S, Lu P, Caldwell H, et al. E2F regulates DDB2: consequences for DNA repair in Rb-deficient cells. *Oncogene.* 2007;26:3572–3581.
26. Chen D, Chen Y, Forrest D, et al. E2f2 induces cone photoreceptor apoptosis independent of E2f1 and E2f3. *Cell Death Differ.* 2013;20:931–940.
27. Xiao F, Zhang W, Chen L, et al. MicroRNA-503 inhibits the G1/S transition by downregulating cyclin D3 and E2F3 in hepatocellular carcinoma. *J Transl Med.* 2013;11:195.